Enzyme I of the Phosphotransferase System: Induced-Fit Protonation of the Reaction Transition State by Cys-502†

Luis Fernando García-Alles,‡ Ignacio Alfonso,§ and Bernhard Erni*,‡

Departement für Chemie und Biochemie, Universität Bern, Freiestrasse 3, CH-3012 Bern, Switzerland, and Departamento de Química Orgánica e Inorgánica, Facultad de Química, Universidad de Oviedo, Julian Claveria, 33071 Oviedo, Spain

Received January 6, 2003; Revised Manuscript Received March 1, 2003

ABSTRACT: Enzyme I (EI), the first component of the phosphoenolpyruvate (PEP):sugar phosphotransferase system (PTS), consists of an N-terminal domain with the phosphorylation site (His-189) and a C-terminal domain with the PEP binding site. Here we use C3-substituted PEP analogues as substrates and inhibitors and the EI(C502A) mutant to characterize structure−activity relationships of the PEP binding site. EI(C502A) is 10 000 times less active than wild-type EI [EI(wt)] with PEP as the substrate, whereas the two forms are equally active with *Z*ClPEP. Cys-502 acts as an acid−base catalyst which stereospecifically protonates the pyruvoyl enolate at C3. The electron-withdrawing chlorine of *Z*ClPEP can compensate for the lack of Cys-502, and in this case, the released 3-Cl-enolate is protonated nonstereospecifically. Several PEP analogues were assayed as inhibitors and as substrates. The respective K_I/K_m ratios vary between 3 and 40 for EI(wt), but they are constant and around unity for EI(C502A). EI(wt) with PEP as the substrate is inhibited by oxalate, whereas EI(C502A) with *Z*ClPEP is not. The different behavior of EI(wt) and EI(C502A) toward the PEP analogues and oxalate suggests that the PEP binding site of EI(wt) exists in a "closed" and an "open" form. The open to closed transition is triggered by the interaction of the substrate with Cys-502. The closed conformation is sterically disfavored by C3-modified substrate analogues such as *Z*ClPEP and *Z*MePEP. If site closure does not occur as with EI(C502A) and bulky substrates, the transition state is stabilized by electron dispersion to the electron-withdrawing substituent at C3.

The phosphoenolpyruvate:sugar phosphotransferase system (PTS)[1] (*1*) mediates the uptake and phosphorylation of carbohydrates, and it controls the metabolism in response to carbohydrate availability. PTSs are widely distributed in eubacteria but absent from eukaryotes. A PTS consists of soluble and membrane proteins. The soluble protein enzyme I (EI) transfers phosphoryl groups from phosphoenolpyruvate (PEP) to the soluble, heat stable protein HPr. HPr in turn donates a phosphoryl group to the sugar-specific membrane transporters (EII^{sugar}). EII consists of two phosphorylation units (IIA and IIB) and one to two membrane-spanning subunits (IIC and IID). The number of different EIIs is species-dependent and is between 1 and 20.

$$PEP \rightarrow EI \rightarrow HPr \rightarrow EIIA^{sugar} \rightarrow EIIB^{sugar} \xrightarrow{EIIC^{sugar}} sugar$$

EI consists of two domains (*2*, *3*). The amino-terminal domain (EIN, residues 1−250) contains His-189, which is transiently phosphorylated by PEP (*4*−*6*). The structure of EIN has been elucidated (*7*, *8*) and its mode of interaction with HPr characterized by NMR spectroscopy (*9*, *10*). It is composed of an HPr-binding α-helical subdomain and an α/β subdomain which is structurally similar to the phosphohistidine swivel domain of pyruvate phosphate dikinase [PPDK (*11*)]. The carboxy-terminal domain, EIC, contains Cys-502, an invariant residue that could be alkylated with *Z*ClPEP (*12*), indicating that it is located in the PEP binding site (*13*). EIC further mediates dimerization (*14*) and confers species and subunit specificity during the phosphoryl transfer to HPr (*15*). Its overall amino acid sequence is homologous to the PEP binding domain of PPDK and other PEP-binding enzymes (*16*). EIC is proteolytically unstable and flexible (*3*), properties that might have prevented its crystallization thus far.

Steady state kinetic (*17*, *18*) and isotope exchange studies (*19*) support a ping-pong mechanism with formation of a covalent phospho-EI intermediate. There exists cumulative evidence that EI is a homodimer and that autophosphorylation of EI by PEP requires the self-associated dimer (*12*, *20*−*24*). The dimer dissociation constant is strongly affected by temperature (*24*, *25*), divalent cations, and PEP (*23*, *26*). The monomer association rate constant is 2−3 orders of magnitude slower than in other dimeric proteins, indicating that dimerization is accompanied by major conformational rearrangements of the interacting EIC domains (*22*, *26*).

Here we employ C3-modified PEP analogues (shown in Chart 1) to investigate the reaction mechanism of EI. The

† This study was supported by Grant 3100-063420 from the Swiss National Science Foundation.

* To whom correspondence should be addressed. Phone: ++41-31-6314346. Fax: ++41-31-6314887. E-mail: erni@ibc.unibe.ch.

‡ Universität Bern.

§ Universidad de Oviedo.

[1] Abbreviations: EI, enzyme I; PEP, phosphoenolpyruvate; PTS, PEP-dependent carbohydrate:phosphotransferase system; *Z*ClPEP, (*Z*)-3-chloro-PEP; *E*ClPEP, (*E*)-3-chloro-PEP; *Z*FPEP, (*Z*)-3-fluoro-PEP; *Z*MePEP, (*Z*)-3-methyl-PEP or (*Z*)-phosphoenolbutyrate; GPDHase, glucose-6-phosphate dehydrogenase; Glc6P, glucose 6-phosphate; PA, proton affinity.

10.1021/bi034007f CCC: $25.00
Published on Web 04/02/2003

Chart 1: Structure of PEP Analogues

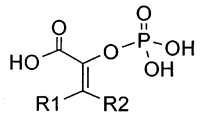

R1	R2	Compound
H	H	PEP
H	F	*Z*FPEP
H	CH_3	*Z*MePEP
H	Cl	*Z*ClPEP
Cl	H	*E*ClPEP

results indicate that Cys-502 of EI and functional groups of the substrate analogue can complement each other and together determine the overall catalytic process. EI binds PEP via an induced-fit mechanism with Cys-502 playing a role not only as a general acid and base but also as the transducer of conformational changes.

MATERIALS AND METHODS

Materials. NADP (sodium salt, Na^+) and 2-oxobutyrate (Na^+) were purchased from Fluka. PEP (cyclohexylammonium salt), β-fluoropyruvate (Na^+), NADH (2 Na^+), bovine heart L-lactate dehydrogenase (LDHase, 525 units/mg), and rabbit muscle pyruvate kinase (lyophilized, 224 units/mg) were from Sigma. Yeast glucose-6-phosphate dehydrogenase (GPDHase, 350 units/mg) was from Boehringer Mannheim. Sephadex DEAE A-25 was from Pharmacia. *Z*- and *E*ClPEP were prepared as described in ref *27*. ^{1}H NMR spectra were recorded at 300.1 MHz. Spectra in D_2O were calibrated against DSS (external standard).

Preparation of ZFPEP and ZMePEP. Four milliliter of a mixture of 50 mM PEP, 500 mM β-fluoropyruvate (or 2-oxobutyrate), 15 mM $MgCl_2$, 1 mM dithiothreitol, and 5 μM EI in 50 mM Tris-HCl (pH 7.4) were incubated at 37 °C for 4 h. The solution was then cooled on ice, loaded on a 2 cm × 15 cm column of Sephadex DEAE A-25 (Cl^- form) at 4 °C, and eluted with a linear KCl gradient (from 0 to 0.4 M, pH 6, 2 mL/min, 10 mL/fraction). Fractions were detected at 254 nm. *Z*MePEP and *Z*FPEP eluted at 0.24 and 0.28 M KCl, respectively. The appropriate fractions were pooled, diluted with 3 volumes of deionized water, and loaded on identical DEAE columns as described above (HCO_3^- form). The products were eluted as described above with triethylammonium bicarbonate (0 to 1 M, pH 8). Fractions containing the products were pooled and lyophilized, yielding the triethylammonium salts of *Z*FPEP (36 mg, 64%) and *Z*MePEP (37 mg, 65%): ^{1}H NMR for *Z*FPEP (CD_3OD) δ 7.45 (1H, dd, J = 75.7, 2.6 Hz, =CHF), 3.17 (8H, q, $NC\underline{H}_2CH_3$), 1.31 (14H, t, $NCH_2C\underline{H}_3$) (*28*); ^{1}H NMR for *Z*MePEP (CD_3OD) δ 6.30 (1H, dq, J = 7.0, 1.8 Hz, =$C\underline{H}CH_3$), 3.17 (8H, q, $NC\underline{H}_2CH_3$), 1.81 (3H, dd, J = 7.0, 2.6 Hz, =$CHC\underline{H}_3$), 1.31 (14H, t, $NCH_2C\underline{H}_3$) (*29*).

Site-Directed Mutagenesis, Overproduction, and Purification of Proteins. Plasmids encoding EI(wt), EI(H189A), and EI(C502A) are described in ref *12*. The EI(H189A/C502A) double mutant was constructed by exchange of restriction fragments between pMSEI189H6 and pMSEI502H6 (*12*). EI(wt), EI(C502A), and EI(H189A/C502A) were expressed in *Escherichia coli* K12 WA2127ΔHIC (*manXYZ ptsIcrr*) which carries a partial deletion of *ptsI*, including the codon for Cys-502 (*30*). EI(H189A) was expressed in *E. coli* TH074 (Δ*ptsI*) which carries a deletion of codons 131−258 of *ptsI* (*31*). Two different strains were used to exclude the formation of wild-type alleles by genetic recombination between the chromosomal and plasmid-born mutant alleles. Such recombination had been found to occur when *ptsI*(C502A) was expressed in TH074 and when *ptsI*(H189A) was expressed in WA2127ΔHIC, leading to a variable degree of low-level contamination of the mutant by wild-type EI. This problem was first not noticed and consequently misinterpreted as EI(H189A) having reduced PTS activity (*12*). EI, HPr, IIA^{Glc}, $IIAB^{Man}$, and $IICB^{Glc}$ were purified as described previously (*30*, *32*). IIC^{Man}/IID^{Man}-containing membranes were prepared as reported previously (*32*), and washed twice by centrifugation and resuspension to free them of membrane-associated cytoplasmic proteins.

Assay for Phosphotransferase Activity. *In vitro* PTS activity was measured as previously described (*12*). Evolution of glucose 6-phosphate (Glc6P) was coupled with its oxidation to 6-phosphoglucono-δ-lactone in a reaction catalyzed by GPDHase. Assay mixtures contained (150 μL per well): 0.7 μM HPr, 1.3 μM $IIAB^{Man}$, 2 μL of $IIC^{Man}IID^{Man}$ membrane extract, 1 mM glucose, 0.7 unit of GPDHase, 1 mM $NADP^+$, 10 mM KCN, and 1 mg/mL BSA in buffer A [100 mM HEPES (pH 7.5), 5 mM DTT, 5 mM NaF, and 5 mM $MgCl_2$]. The concentrations of EI and PEP (analogue) are given in the figure legends. The EI concentration was kept rate-limiting. The reaction rates were <10% of the maximum attainable with a saturating concentration of EI. The reactions were started by addition of 20 μL of PEP (analogue) in buffer A to the assay mixture (130 μL/well) containing the rest of the components preincubated for 10 min at 30 °C. The inhibition assays were started by the addition of 20 μL of mixtures containing the phosphoryl donor and the inhibitor in buffer A.

Quantum Mechanical Calculations. The theoretical proton affinities (PA) for each of the C3-modified enolates were determined using both semiempirical and *ab initio* methods. The PA of a base, B, is defined as the negative of the gas phase heat of reaction of its protonation, that is

$$\mathrm{PA} = -[\Delta H_f(\mathrm{BH}^+) - \Delta H_f(\mathrm{B}) - \Delta H_f(\mathrm{H}^+)] \quad (1)$$

$\Delta H_f(BH^+)$ and $\Delta H_f(B)$ correspond to the heats of formation of the C3-substituted pyruvic acid and its enolate, respectively. They were calculated using the PM3 semiempirical method (*33*). Full geometric optimizations started from the carboxylate-protonated and -conjugated planar structures of the C3-modified pyruvoyl enolates and the corresponding pyruvic derivatives obtained by protonation at C3 from the 2-*re* face. They were first minimized by molecular mechanics (MMX), and subsequently optimized at the semiempirical level of theory. The energies of the closest local minima were evaluated and taken into account for the calculation of PA values. The experimental value for the heat of formation for the proton [$\Delta H_f(H^+)$ = 367.2 kcal/mol] was used (*34*).

Using *ab initio* methods, the PA is defined by the equation

$$\mathrm{PA} = -\{H(\mathrm{BH}^+) - [H(\mathrm{B}) + {}^5/_2RT]\} \quad (2)$$

where H is the computed sum of electronic and thermal enthalpies with zero-point energy (ZPE) corrections and ${}^5/_2RT$ is the proton contribution to C_p (ideal gas). The same initial structures used for semiempirical calculations were fully

optimized at the *ab initio* (STO-3G) level. Frequency analysis showed that all the optimized structures were energy minima. These structures were subjected to a thermochemical analysis. ZPE was computed for every optimized geometry, and the thermal correction in the energy value was used to calculate the enthalpies at 298 K, with the ZPE correction.

Stereospecificity of EI-Dependent Substrate Protonation. The EI reaction mixture in 0.6 mL of D_2O contained 10 mM *Z*MePEP, 3 μM EI(wt) [or 10 mM *Z*ClPEP and 7 μM EI(C502A)], 0.7 μM HPr, 1.3 μM $IIAB^{Man}$, 1 μL of $IIC^{Man}IID^{Man}$ membrane extract, 10 mM glucose, 12 mM NADH, 100 units of bovine heart LDHase, 20 mM KCN, 100 mM phosphate buffer (pD 7.5), 1 mM DTT, 5 mM NaF, and 2 mM $MgCl_2$. The pyruvate kinase reaction mixture contained 10 mM PEP analogue, 11 mM ADP, 400 units of pyruvate kinase, 11 mM NADH, 100 units of bovine heart LDHase in 100 mM phosphate buffer (pD 7.5), 100 mM KCl, and 5 mM $MgCl_2$. The reaction mixtures were incubated for 2 h at 30 °C. The pD of the mixture was adjusted to <2 with 90 μL of HCl (1 M), and the solution was lyophilized. Three milliliters of MeOH was added, and the solution was sonicated for 10 s and filtered through cotton. After solvent evaporation, the residue was redissolved in 5 mL of a 4:1 $CHCl_3$/MeOH mixture, sonicated, kept for 2 h at 4 °C, and again filtered and freed of solvent by evaporation. The resulting residue was dissolved in $CDCl_3$ or D_2O and analyzed by ^{1}H NMR.

RESULTS

EI-Catalyzed Synthesis of ZFPEP and ZMePEP. Phospho-EI can transfer its phosphoryl group to pyruvate and to β-substituted pyruvate derivatives (*35*, *36*). We have exploited EI's phosphotransferase activity to prepare pure *Z*FPEP and *Z*MePEP from 3-fluoropyruvate and 2-oxobutyrate, respectively. The approach to equilibrium of the exchange reaction was followed by ^{1}H NMR. The reaction was carried out in the presence of a 10-fold molar excess of the oxo compounds over PEP to facilitate the product separation by anion exchange chromatography.

Dimerization of EI. The EI concentrations used in the assays below varied between 5 nM and 15 μM depending on the specific activity of the EI mutant for a given substrate analogue. In this range, the variation of the EI monomer: dimer ratio cannot be neglected, and it might affect the values of the kinetic constants. To estimate what effect a variable monomer−dimer distribution might maximally have on the specific activity, V_{max} of EI(wt) was determined in the presence of increasing concentrations of inactive EI mutants. The concentration of EI(wt) was 1 nM, where EI is assumed to be completely monomeric, and EI(wt) was then driven into the (hetero) dimeric form with inactive EI (Figure 1). V_{max} of EI(wt) increased up to 10-fold upon addition of EI(H189A), EI(C502A), or the double mutant, consistent with results obtained by Seok et al. (*20*) with mixtures between EI(wt) and the EI(H189G) or EI(G338D) mutant. Mixtures of EI(H189A) and EI(C502A) were completely inactive (not shown). This indicates that activation of EI in the dimer is only allosteric and not due to extra catalytic activity supplied by the intact domain of a mutant subunit. It further indicates that the functional catalytic unit is contained in a single subunit and cannot be formed between domains on different subunits.

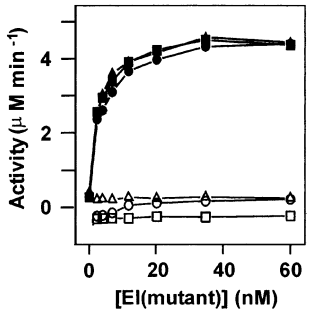

FIGURE 1: Phosphotransferase activity of EI(wt)−EI(mutant) heterodimers. Stimulation of EI(wt) activity by EI(H189A) (●), EI(C502A) (■), and EI(H189A/C502A) (▲). The background activities of EI(H189A), EI(C502A), and EI(H189A/C502A) measured in the absence of EI(wt) are shown with open symbols. [EI(wt)] = 1 nM. EI mixtures were preincubated for 15 min at 30 °C, and the reaction was then started by the addition of PEP to a concentration of 1 mM. EII^{Man} was used as the terminal phosphotransferase, and Glc6P was detected with GPDHase.

Table 1: Kinetic Data from PEP Analogues as Phosphoryl Donors to EI[a]

substrate	[EI] (μM)	K_m (mM)	k_{cat} (min^{-1})	k_{cat}/K_m (mM^{-1} min^{-1})
		Wild-Type EI		
PEP	0.005	0.14 ± 0.01	3830 ± 60	27000 ± 2000
*Z*FPEP	0.006	0.11 ± 0.02	370 ± 30	3400 ± 800
*Z*MePEP	0.024	0.43 ± 0.01	285 ± 3	660 ± 20
*Z*ClPEP[b]	3	0.036 ± 0.005	12.8 ± 0.4	350 ± 60
*Z*ClPEP[c]	3	0.025 ± 0.002	15.8 ± 0.3	630 ± 60
*E*ClPEP	15	0.12 ± 0.02	2.8 ± 0.2	23 ± 5
		EI C502A Mutant		
PEP	5	0.041 ± 0.006	0.35 ± 0.01	8 ± 2
*Z*FPEP	5	0.035 ± 0.004	1.5 ± 0.04	43 ± 6
*Z*MePEP	9	ND[d]	<0.05	ND[d]
*Z*ClPEP	0.8	0.054 ± 0.005	10.8 ± 0.3	200 ± 20
*E*ClPEP	15	0.13 ± 0.02	0.54 ± 0.02	4.2 ± 0.8

[a] PTS activity was measured at 30 °C in the presence of 0−1 mM PEP analogue, at the specified rate-limiting EI concentration. The initial rate dependence on the concentration was fitted by nonlinear regression to a hyperbola to derive the kinetic constants. [b] Without correction for slow suicide inactivation of EI by *Z*ClPEP. [c] With correction for concomitant suicide inactivation. Progress curves measured at eight different *Z*ClPEP concentrations were simultaneously fitted [DynaFit (*43*)] to a Michaelis−Menten model, including irreversible inhibition. K_m, k_{cat}, and the first-order inactivation rate constant (k^{inact}) were left as adjustable parameters. A k^{inact} of 0.62 ± 0.03 min^{-1} was determined from such a fit. [d] Could not be determined.

Figure 1 shows that EI is dimeric at total concentrations above 20 nM, where k_{cat} and K_m become concentration independent (k_{cat} = 5650 min^{-1}, K_m = 0.09 μM). The catalytic constants of EI(wt) for PEP and ZFPEP, which were measured at 5 nM EI (below) might therefore be underestimated.

Catalytic Activity of EI(wt) and Active Site Mutants. EI(wt) and EI(C502A) can utilize several C3-modified PEP analogues (shown in Chart 1) as alternative phosphoryl donors. The kinetic constants of EI for these substrates are listed in Table 1. The Michaelis constants (K_m) for EI(wt) and EI(C502A) are of the same order of magnitude, and they vary little (<6-fold), indicating that the two EIs have comparable affinities for the different PEP analogues. The turnover numbers (k_{cat}), however, are very different. The k_{cat} of EI(wt) for PEP is 10000-fold larger than the k_{cat} of EI(C502A). The k_{cat} values moreover vary with the physi-

cochemical properties of the substrate. The k_{cat} of EI(wt) decreases more than 1000-fold with an increase in the size and electronegativity of the substituent at C3 (H > F > CH_3 ≫ Cl). In contrast, the k_{cat} of EI(C502A) increases for substrates with electronegative substituents, so much that the k_{cat} of EI(C502A) and the k_{cat} of EI(wt) for *Z*ClPEP become almost identical. This suggests that Cys-502 is essential as a general acid−base catalyst for the reaction of PEP, consistent with the earlier observations that phosphorylation of EI by PEP is accompanied by a proton transfer from the enzyme to C3 of PEP, and that EI is inactivated by reaction of 3-bromopyruvate with a cysteine (*12*, *19*, *37*). Cys-502 is dispensable for the reaction of *Z*ClPEP because the chlorine at C3 partially compensates for the loss of acid−base catalysis, most likely by increasing the dispersion of negative charge in the enolate-like transition state. The second EI(H189A) active site mutant and the EI(H189A/C502A) double mutant are inactive with all substrates (see Materials and Methods).

Effects of Cys-502 and Substrate Modifications on the Reaction Rate. The k_{cat} of EI(C502A) for *Z*ClPEP is 30-fold larger than for PEP (Table 1), indicating that chlorine at C3 compensates for the loss of acid−base catalysis. If so, a correlation should exist between the difference of activation energies of reactions catalyzed by EI(C502A) and by EI(wt) with different C3-modified PEP analogues [$\Delta\Delta G^{\#}$(C502A−wt) for an analogue] and the proton affinity (PA) of the enolate of these analogues. These PAs are determined by the substituents at C3.

The difference $\Delta\Delta G^{\#}$(C502A−wt) [=$\Delta G^{\#}$(C502A) − $\Delta G^{\#}$(wt)] is a measure of the contribution of Cys-502 to the stabilization of the transition state. The $\Delta G^{\#}$ values were calculated from the experimental k_{cat}/K_m values using the following equation (*38*):

$$\Delta G^{\#} = -RT \ln[(k_{cat}/K_m)(h/\kappa T)] \qquad (3)$$

Here it is assumed that the Cys → Ala substitution alone does not significantly alter the environment in the active site, and that the substituents at C3 exert similar steric perturbations upon EI(wt) and EI(C502A) so that their effects cancel in $\Delta\Delta G^{\#}$(C502A−wt).

The theoretical PA values of the different enolates were calculated using semiempirical (PM3) and *ab initio* (STO-3G) quantum mechanical methods (see Materials and Methods). Full geometric optimizations were carried out on each C3-modified pyruvoyl enolate and on the correspoding pyruvic derivatives obtained by protonation at C3 from the 2-*re* face. The energies of the closest local minima were then used to calculate the PA values. The coordinates and energies are given as Supporting Information.

The calculated PA of each C3-modified pyruvoyl enolate and the experimentally determined $\Delta\Delta G^{\#}$(C502A−wt) are listed in Table 2. Replacement of Cys-502 with Ala causes increasing destabilization of the transition state of the reaction in the following order: H ≈ CH_3 > F ≫ *E*Cl > *Z*Cl. The effect of Cys-502 on catalysis [$\Delta\Delta G^{\#}$(C502A−wt)] directly correlates with the theoretical PA of the enolate released from each substrate during catalysis. The higher the PA of the enolate intermediate (and consequently the higher its instability), the higher the importance of Cys-502 for catalysis.

Table 2: Stabilization of the Reaction Transition State by Cys-502 of EI

substrate	$\Delta\Delta G^{\#}$(C502A−wt)[a]	PA (STO-3G)[b]	PA (PM3)[b]
PEP	4.9	452.4	347.1
*Z*FPEP	2.6	441.7	335.9
*Z*MePEP	>5	449.6	346.0
*Z*ClPEP	0.69	430.1	334.6
*E*ClPEP	1.0	433.7	335.8

[a] Calculated from the values of k_{cat}/K_m in Table 1, using the equation $\Delta\Delta G^{\#}$(C502A−wt) = $-RT \ln[(k_{cat}/K_m)^{C502A}/(k_{cat}/K_m)^{wt}]$. Units are kilocalories per mole. [b] Proton affinity of the enolate released from the indicated substrate. Units are kilocalories per mole. Calculated by quantum mechanical methods, as described in Materials and Methods.

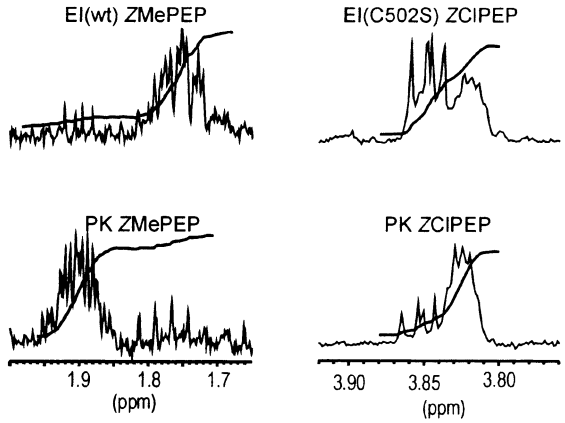

FIGURE 2: Stereospecificity of deuteration in reactions with EI. ^{1}H NMR spectrum of (2*S*)-3-methyllactate (in $CDCl_3$) and (2*S*)-3-Cl-lactate (in D_2O, pD 7.5) formed in reactions with EI(wt) and EI(C502A) (top panels) or pyruvate kinase (PK, bottom panels). Only the NMR regions corresponding to the C3 methylene protons are shown. In four parallel reactions, *Z*ClPEP and *Z*MePEP were incubated with EI and pyruvate kinase. The reaction products, 3-Cl-pyruvate and 3-methylpyruvate, were reduced enzymatically with bovine heart LDHase to afford the 2*S*-diastereoisomers which could then be characterized by ^{1}H NMR spectroscopy.

This correlation adds evidence for the role of Cys-502 as a proton donor during catalysis.

Stereospecificity of Protonation of ZClPEP. Robillard and co-workers demonstrated that EI protonates *Z*MePEP stereospecifically from the 2-*re*, 3-*si* face and that protonation involves a noninterchangeable proton from the active site (*35*, *39*). In contrast, protonation of the enolate produced from *Z*ClPEP in the reaction with EI(C502A) is nonstereospecific as shown below.

Phosphotransferase reactions were carried out in D_2O with (*Z*)-3-Cl-[3-H]PEP and EI(C502A) to afford 3-Cl-[3-H]-pyruvate and with (*Z*)-3-Me-[3-H]PEP and EI(wt) to afford 2-oxo-[3-H]butyrate. The reaction products were resolved into diastereoisomers by *in situ* reduction with lactate dehydrogenase. For reference and as a control that the PEP analogues do not racemize spontaneously, *Z*ClPEP and *Z*MePEP were also reacted with pyruvate kinase, which is known to stereospecifically protonate PEP from the 2-*si*, 3-*re* face (*35*, *39*). The diastereoisomers were then characterized by ^{1}H NMR spectroscopy (Figure 2). The integrals over the signals of the C3 protons of the two α-hydroxybutyrate diastereomers produced in the reaction with EI(wt) are very different, indicative of stereospecific protonation from the 2-*re*, 3-*si* side. The signal intensities of the products formed

with pyruvate kinase are also different, but in the opposite sense. In contrast, the integrals of the 3-Cl-lactate proton signals are comparable when *Z*ClPEP reacts in the presence of EI(C502A). This indicates that the enolate of 3-Cl-pyruvate is protonated from both sides, most likely only after its release into the aqueous medium. The protonation stereospecificity of EI(wt) for *Z*ClPEP could not be determined experimentally because *Z*ClPEP is a suicide inhibitor which prevents the generation of enough product for NMR analyses. However, in view of the almost identical kinetic constants of EI(wt) and EI(C502A) for *Z*ClPEP (Table 1, and below) a similar, i.e., nonstereospecific, reaction mechanism can be assumed for the wild type and mutant. This lack of stereospecificity of EI(C502A) for *Z*ClPEP also indicates that no other ionizable residue which could act as a general acid and/or base (proton donor) instead of Cys-502 is close enough to the enolate. From this experiment, it is clear that Cys-502 acts as a general acid and/or base. But this is not its only function as indicated in the following section.

Inhibition of EI by PEP Analogues and Oxalate. PEP analogues for which EI has a low k_{cat} (Table 1) were used as inhibitors of EI activity. PEP and *Z*ClPEP were used as substrates of EI(wt) and EI(C502A), respectively, in these experiments. Inhibition was competitive, as shown for *Z*FPEP and *Z*MePEP in panels A, B, and D of Figure 3. The inhibition constants (K_I) are given in Table 3. The K_I of EI(C502A) is 1 order of magnitude smaller (15−30-fold) than the K_I of EI(wt). The K_I/K_m ratios of EI(C502A) are nearly constant and close to unity for all PEP analogues. In contrast, the K_I/K_m ratios of EI(wt) vary considerably for the different analogues, from 3 for *Z*ClPEP to 40 for *E*ClPEP (Table 3). This fair correlation between K_I and K_m of EI(C502A) and the lack of correlation for EI(wt) together indicate that EI(wt) and EI(C502A) follow two qualitatively different reaction mechanisms with the one followed by EI(wt) being the more complex.

A qualitative difference between EI(wt) and EI(C502A) is also seen when inhibition by oxalate is compared. Oxalate is a good inhibitor of several PEP-utilizing enzymes (*40*, *41*). It mimics the charge distribution of the pyruvoyl enolate, and inhibition therefore is diagnostic for a phosphoryl transfer reaction involving the formation of an enolate intermediate. Inhibition by oxalate was assayed in the presence of PEP and different C3-modified PEP analogues as the reacting substrates. It was of the mixed type whereby oxalate interacted more strongly with the free enzyme (represented by K_{I1}) than with the covalent phospho-EI intermediate (K_{I2}) (Table 4). Interestingly, inhibition by oxalate depended on which compound was used as the substrate in the assay. Inhibition of EI(wt) by oxalate was strongest with PEP as the substrate (Figure 3E), moderate with *Z*FPEP and *Z*MePEP, and zero with *Z*ClPEP. Like EI(wt), EI(C502A) was moderately inhibited when *Z*FPEP and not when *Z*ClPEP was the substrate (Table 4 and Figure 3F). PEP could not be used because it is an excessively poor substrate for EI(C502A).

Inhibition of EI(wt) and inhibition of EI(C502A) are differently affected by the size and chemical properties of the inhibitors. EI(wt) is strongly inhibited by the small oxalate but not by the sterically demanding *Z*MePEP (Figure 3C,E) and *E*ClPEP (Table 3), whereas EI(C502A) is strongly inhibited by *E*ClPEP (Table 3) and *Z*MePEP but not by the smaller oxalate (compare panels D and F of Figure 3), pointing again to a qualitative difference between the PEP binding sites of EI(wt) and EI(C502A).

Finally, this difference is also evident from how the different analogues protect against *Z*ClPEP-mediated suicide

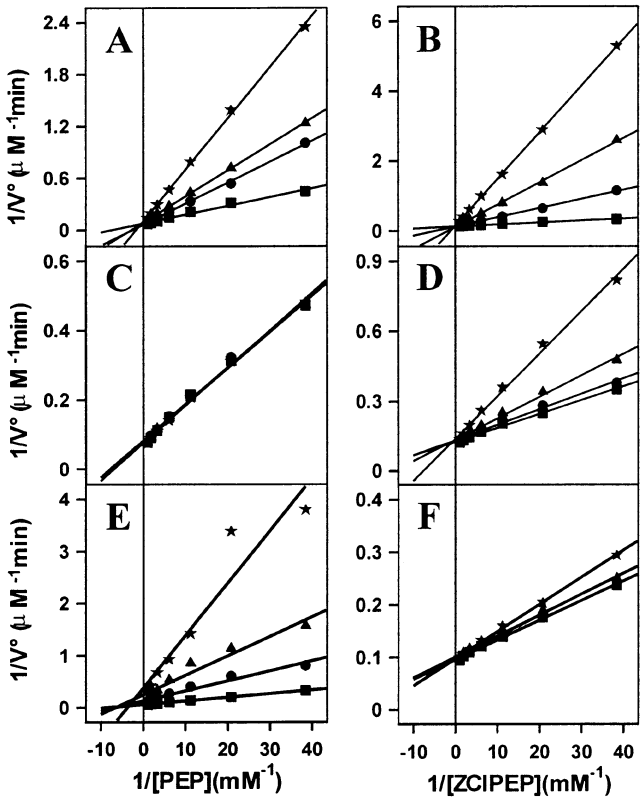

FIGURE 3: Inhibition of EI by PEP analogues and oxalate. Shown are Lineweaver−Burk plots of inhibition kinetics: (A, C, and E) EI(wt) with PEP as the substrate and (B, D, and F) EI(C502A) with *Z*ClPEP as the substrate. The inhibitors were *Z*FPEP (A and B), *Z*MePEP (C and D), and oxalate (E and F). Concentrations were as follows: 4.8 nM EI(wt) in panels A, C, and E, 0.77 μM EI(C502A) in panels B and D, and 1.5 μM EI(C502A) in panel F. *Z*FPEP and *Z*MePEP concentrations were as follows: 0 (■), 0.12 (●), 0.37 (▲), and 1.1 mM (★) in panels A and C and 0 (■), 0.06 (●), 0.14 (▲), and 0.55 mM (★) in panels B and D. Oxalate concentrations were as follows: 0 (■), 0.056 (●), 0.17 (▲), and 0.50 mM (★). EII^{Man} was used as the terminal phosphotransferase.

Table 3: Inhibition of EI by PEP Analogues[a]

	EI(wt)[b]		EI(C502A)[c]	
inhibitor	K_I (mM)	K_I/K_m	K_I (mM)	K_I/K_m
PEP	−	−	0.07 ± 0.04	1.7
*Z*FPEP	0.48 ± 0.09	4.4	0.030 ± 0.004	1.2
*Z*MePEP	>5	>12	0.20 ± 0.03	ND
*Z*ClPEP	0.08 ± 0.03	3.2	−	−
*E*ClPEP	4.6 ± 0.9	38	0.17 ± 0.03	1.3

[a] PTS activity was measured at eight concentrations of the phosphoryl donor (0−1 mM) in the presence of four fixed concentrations of the inhibitor (as in Figure 3A−D). The K_m^{app} and V_{max}^{app} values for the phosphoryl donor at each inhibitor concentration were then determined by a nonlinear regression fit to a Michaelis−Menten hyperbola. The K_I values were obtained by linear regression to the equation $K_m^{app} = K_m(1 + [I]/K_I)$. The K_m for the calculation of the K_I/K_m ratio is taken from Table 1. [b] PEP as the substrate in the presence of 4.8 nM EI(wt). [c] *Z*ClPEP as the substrate using 0.77 μM EI(C502A).

Table 4: Inhibition of EI by Oxalate[a]

substrate	[EI] (μM)	K_S (mM)	k_{cat} (min^{-1})	K_{I1} (mM)	K_{I2} (mM)
		EI(wt)			
PEP	0.005	0.14	3800	0.019	0.28
*Z*FPEP	0.013	0.093	400	0.35	1.9
*Z*MePEP	0.032	0.67	390	0.45	0.19
*Z*ClPEP[b]	1.3	0.024	8	>5	>5
		EI(C502A)[c]			
*Z*FPEP	5	0.033	1.5	0.59	>5
*Z*ClPEP	1.5	0.040	7	1.2	>5

[a] PTS initial rates were measured at the indicated EI concentrations, at eight substrate concentrations (0−1 mM), in the presence of three or four fixed concentrations of oxalate (0−0.5 mM). The kinetic constants were obtained from the initial rates by fitting the data points to a mixed-type inhibition model using DynaFit (*43*). [b] Initial rates were calculated from progress curves recorded for the first 2 min of reaction. [c] The low activity of EI(C502A) with PEP and *Z*MePEP as substrates precluded an accurate determination of K_I.

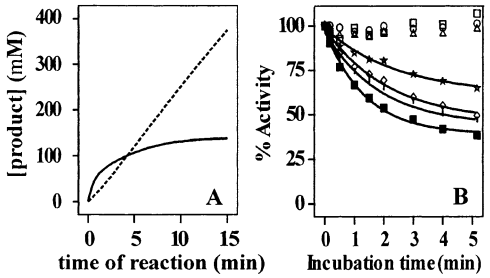

FIGURE 4: Suicide inhibition of EI by *Z*ClPEP. (A) Progress curves of Glc phosphorylation by 4 μM EI(wt) (—) and 3 μM EI(C502A) (- - -) in the presence of 1 mM *Z*ClPEP. Glc6P was detected with GPDHase. (B) Protection of EI(wt) from inactivation by *Z*ClPEP. EI(wt) (5 μM) was incubated at 30 °C without *Z*ClPEP (□), with 0.1 mM *Z*ClPEP alone (■), and with ZClPEP together with 1 mM protecting compound: PEP (○), *Z*FPEP (△), *Z*MePEP (☆), *E*ClPEP (◇), and oxalate (|). Multiple turnovers were maintained by adding catalytic amounts of HPr, $IIAB^{Man}$, and membranes containing $IIC^{Man}IID^{Man}$, 5 mM Mg^{2+}, 5 mM DTT, 1 mg/mL BSA, and 1 mM glucose. To stop the progress of suicide inhibition, aliquots were taken at the indicated time points and diluted into cold buffer containing 2 mM PEP. The EI residual activity was then determined in a standard PTS assay.

inhibition of EI. 3-Cl-pyruvate, which is formed from *Z*ClPEP at the same time as or after phosphoryl transfer to His-189, reacts with the Cys-502 and thereby irreversibly inactivates EI (*12*). The progress curve of the EI-dependent formation of Glc6P shows that inactivation by *Z*ClPEP is not instantaneous but occurs at a rate of one hit per 30 turnovers (Figure 4A). In the presence of EI(C502A) instead of EI(wt), formation of Glc6P is constant over time, indicating that 3-Cl-pyruvate does not react with any other essential residue of EI or of any other PTS protein. PEP and *Z*FPEP, in 10-fold molar excess over *Z*ClPEP, fully protect EI(wt) against inactivation by *Z*ClPEP, whereas oxalate, *Z*MePEP, and *E*ClPEP provide only partial protection (Figure 4B). The efficiency of protection decreases in the following order: PEP ≥ *Z*FPEP ≫ *Z*MePEP > *E*ClPEP > oxalate. Oxalate, which is a strong inhibitor of EI(wt) when PEP is used as the substrate (Figure 3E), almost completely fails to protect EI(wt) against inactivation by *Z*ClPEP, suggesting that PEP and *Z*ClPEP react with two different conformational states of the EI active site.

DISCUSSION

The main conclusion of this study with EI(wt) and EI(C502A) and their reactivity toward C3-modified PEP analogues is that Cys-502 of EI has two functions. (i) It serves as a general acid and/or base in the PEP binding site of EI, and (ii) it mediates the induced fit between the enzyme and substrate in a way which is sensitive to the stereoelectronic property of the substrate. The quality of the fit between the enzyme and substrate in the transition state then affects the overall catalytic activity of EI.

Cys-502 is essential for activity with PEP, but dispensable with *Z*ClPEP. The contribution of Cys-502 to catalysis [$\Delta\Delta G^{\#}$(C502A−wt)] with different PEP analogues and the stability of the released enolates, defined by the quantum mechanically calculated proton affinities, are inversely correlated. The reaction transition state, electronically similar to the enolate, can thus be stabilized by either Cys-502-dependent protonation at C3 or electron dispersion by an electron-withdrawing substituent at C3. The stereospecificity of deuteration of the pyruvoyl enolate and the nonstereospecificity with *Z*Cl-pyruvoyl enolate indicate that Cys-502 acts as the (only) acid or base catalyst.

The results can be rationalized with a working model for a PEP binding site with the following properties. In the absence of substrate, EI does not have a structure complementary to the substrate in the transition state. Cys-502 becomes aligned in the optimal orientation for catalysis only during approach to the transition state. The great difference in k_{cat}/K_m but similarity of K_m of EI for the PEP analogues are consistent with the notion that substrate binding energy is used to distort the enzyme (*38*). The high-energy transition state formed in the reaction with PEP triggers the movement of Cys-502 toward the C3 atom, resulting in a lower-energy closed conformation. Active site closure is favored by the small size of the pyruvoyl enolate. The transition state formed in the reaction with *Z*ClPEP is stabilized by the electronegative substituent and therefore lower in energy. Active site closure is disfavored by the larger size of the *Z*Cl-pyruvoyl enolate, and therefore, less energy can be gained by site closure. The self-stabilizing *Z*ClPEP can react in the open conformation of the active site and therefore does not or only rarely contacts Cys-502. This aspect of the model is supported by the following observations. (i) Proton transfer and the electronegative effect are not additive when *Z*ClPEP is used as the substrate because the bulky chlorine prevents the induced fit that is necessary to bring the Cys-SH in juxtaposition with C3 of the substrate. (ii) EI(wt) and EI(C502A) have comparable activities toward *Z*ClPEP because both have to react with the active site in the open conformation to accommodate this bulky substrate. (iii) EI(wt) is inactivated only slowly by one in 30 turnovers because Cys-502 is not readily accessible when the active site is in the open conformation. *Z*MePEP is of particular interest because the methyl group is bulky but not electronegative. Activation of *Z*MePEP requires closure of the binding site which is disfavored by the size of the substrate in its ground state. As a consequence, K_m of EI(wt) for *Z*MePEP is 10 times higher than for *Z*ClPEP. *Z*MePEP and *Z*ClPEP are isosteric, their approach to Cys-502 being similarly compromised, but whereas *Z*MePEP must exert extra stress upon the enzyme to reach Cys-502 and close the site, *Z*ClPEP

does not. In contrast to the PEP analogues, oxalate is smaller than PEP and as a mimic of the enolate binds strongly to the closed state only. It inhibits EI(wt) with substrates which require a closed state of the active site (Figure 3E). Oxalate does not bind to the open state and therefore also does not inhibit EI(wt) and EI(C502A) from reacting with substrates which require an active site in the open conformation.

Here, a conformation change of the region around Cys-502 is proposed on the basis of enzyme kinetic arguments. That this region must be mobile was concluded previously from a change in Trp-498 fluorescence intensity which occurs upon dimerization of EI (*22*). By using fluorescence energy transfer to an acceptor bound to Cys-502, it was shown that Cys-502 is in the proximity of Trp-498 (*22*). Mobility of Cys-502 may be contingent on the glycines which flank the active site Cys on both sides and which are invariant in all EI homologues (*12*). Such an induced-fit mechanism involving the active site cysteine has been firmly established by enzyme kinetics as well as by X-ray crystallography for MurA, a PEP-utilizing enzyme displaying a similar motif, a cysteine in a loop between glycines (*42*).

SUPPORTING INFORMATION AVAILABLE

Cartesian coordinates for all the optimized structures, energies in atomic units (PM3), and thermochemical analysis (STO-3G). This material is available free of charge via the Internet at http://pubs.acs.org.

REFERENCES

1. Postma, P. W., Lengeler, J. W., and Jacobson, G. R. (1996) in *Escherichia coli and Salmonella: cellular and molecular biology* (Neidhardt, F. C., et al., Eds.) pp 1149−1174, ASM Press, Washington, DC.
2. Lee, B. R., Lecchi, P., Pannell, L., Jaffe, H., and Peterkofsky, A. (1994) *Arch. Biochem. Biophys. 312*, 121−124.
3. LiCalsi, C., Crocenzi, T. S., Freire, E., and Roseman, S. (1991) *J. Biol. Chem. 266*, 19519−19527.
4. Alpert, C. A., Frank, R., Stueber, K., and Deutscher, J. H. (1985) *Biochemistry 24*, 959−964.
5. Garrett, D. S., Seok, Y. J., Peterkofsky, A., Clore, G. M., and Gronenborn, A. M. (1998) *Protein Sci. 7*, 789−793.
6. Weigel, N., Kukuruzinska, M. A., Nakazawa, A., and Waygood, E. B. R. S. (1982) *J. Biol. Chem. 257*, 14477−14491.
7. Liao, D. I., Silverton, E., Seok, Y. J., Lee, B. R., Peterkofsky, A., and Davies, D. R. (1996) *Structure 4*, 861−872.
8. Garrett, D. S., Seok, Y. J., Liao, D. I., Peterkofsky, A., Gronenborn, A. M., and Clore, G. M. (1997) *Biochemistry 36*, 2517−2530.
9. Garrett, D. S., Seok, Y. J., Peterkofsky, A., Clore, G. M., and Gronenborn, A. M. (1997) *Biochemistry 36*, 4393−4398.
10. Garrett, D. S., Seok, Y. J., Peterkofsky, A., Gronenborn, A. M., and Clore, G. M. (1999) *Nat. Struct. Biol. 6*, 166−173.
11. Herzberg, O., Chen, C. C., Kapadia, G., McGuire, M., Carroll, L. J., Noh, S. J., and Dunaway-Mariano, D. (1996) *Proc. Natl. Acad. Sci. U.S.A. 93*, 2652−2657.
12. Garcia-Alles, L. F., Flükiger, K., Hewel, J., Gutknecht, R., Siebold, C., Schürch, S., and Erni, B. (2002) *J. Biol. Chem. 277*, 6934−6942.
13. Seok, Y. J., Lee, B. R., Gazdar, C., Svenson, I., Yadla, N., and Peterkofsky, A. (1996) *Biochemistry 35*, 236−242.
14. Zhu, P. P., Szczepanowski, R. H., Nosworthy, N. J., Ginsburg, A., and Peterkofsky, A. (1999) *Biochemistry 38*, 15470−15479.
15. Seok, Y. J., Lee, B. R., Zhu, P. P., and Peterkofsky, A. (1996) *Proc. Natl. Acad. Sci. U.S.A. 93*, 347−351.
16. Pocalyko, D. J., Carroll, L. J., Martin, B. M., Babbitt, P. C., and Dunaway-Mariano, D. (1990) *Biochemistry. 29*, 10757−10765.
17. Weigel, N., Waygood, E. B., Kukuruzinska, M. A., and Nakazawa, A. R. (1982) *J. Biol. Chem. 257*, 14461−14469.
18. Waygood, E. B., and Steeves, T. (1980) *Can. J. Biochem. 58*, 40−48.
19. Hoving, H., Lolkema, J. S., and Robillard, G. T. (1981) *Biochemistry 20*, 87−93.
20. Seok, Y. J., Zhu, P. P., Koo, B. M., and Peterkofsky, A. (1998) *Biochem. Biophys. Res. Commun. 250*, 381−384.
21. Misset, O., Brouwer, M., and Robillard, G. T. (1980) *Biochemistry 19*, 883−890.
22. Han, M. K., Knutson, J. R., Roseman, S., and Brand, L. (1990) *J. Biol. Chem. 265*, 1996−2003.
23. Dimitrova, M. N., Szczepanowski, R. H., Ruvinov, S. B., Peterkofsky, A., and Ginsburg, A. (2002) *Biochemistry 41*, 906−913.
24. Chauvin, F., Brand, L., and Roseman, S. (1994) *J. Biol. Chem. 269*, 20263−20269.
25. Kukuruzinska, M. A., Turner, B. W., Ackers, G. K., and Roseman, S. (1984) *J. Biol. Chem. 259*, 11679−11681.
26. Chauvin, F., Brand, L., and Roseman, S. (1996) *J. Biol. Chem. 269*, 20270−20274.
27. Garcia-Alles, L. F., and Erni, B. (2002) *Eur. J. Biochem. 269*, 3226−3236.
28. Stubbe, J. A., and Kenyon, G. L. (1972) *Biochemistry 11*, 338−345.
29. Duffy, T. H., Saz, H. J., and Nowak, T. (1982) *Biochemistry 21*, 132−139.
30. Stolz, B., Huber, M., Markovic-Housley, Z., and Erni, B. (1993) *J. Biol. Chem. 268*, 27094−27099.
31. Hesterkamp, T., and Erni, B. (1999) *J. Mol. Microbiol. Biotechnol. 1*, 309−317.
32. Mao, Q., Schunk, T., Flükiger, K., and Erni, B. (1995) *J. Biol. Chem. 270*, 5258−5265.
33. Stewart, J. J. P. (1989) *J. Comput. Chem. 10*, 209−220.
34. Lias, S. G., Bartmess, J. E., Liebman, J. F., Holmes, J. L., Levin, R. D., and Maillard, W. G. (1988) *J. Phys. Chem. Ref. Data, Suppl. 17*, 861.
35. Hoving, H., Nowak, T., and Robillard, G. T. (1983) *Biochemistry 22*, 2833−2838.
36. Saier, M. H., Schmidt, M. R., and Lin, P. (1980) *J. Biol. Chem. 255*, 8579−8584.
37. Hoving, H., ten Hoeve Duurkens, R., and Robillard, G. T. (1984) *Biochemistry 23*, 4335−4340.
38. Fersht, A. (1999) *Structure and mechanism in protein science: a guide to enzyme catalysis and protein folding*, W. H. Freeman, New York.
39. Hoving, H., Crysell, B., and Leadlay, P. F. (1985) *Biochemistry 24*, 6163−6169.
40. Seidel, H. M., and Knowles, J. R. (1994) *Biochemistry 33*, 5641−5646.
41. Reed, G. H., and Morgan, S. D. (1974) *Biochemistry 13*, 3537−3541.
42. Schonbrunn, E., Eschenburg, S., Krekel, F., Luger, K., and Amrhein, N. (2000) *Biochemistry 39*, 2164−2173.
43. Kuzmic, P. (1996) *Anal. Biochem. 237*, 260−273.

BI034007F